Design, Fabrication, and Testing of a Hybrid CMOS/PDMS Microsystem for Cell Culture and Incubation

Jennifer Blain Christen, *Student Member, IEEE*, and Andreas G. Andreou, *Fellow, IEEE*

Invited Paper

***Abstract*—We discuss the design, fabrication, and testing of a hybrid microsystem for stand-alone cell culture and incubation. The micro-incubator is engineered through the integration of a silicon CMOS die for the heater and temperature sensor, with multilayer silicone (PDMS) structures namely, fluidic channels and a 1.5-mm diameter 12-μL culture well. A 90-μm-thick PDMS membrane covers the top of the culture well, acting as barrier to contaminants while at the same time allowing the cells to breath and exchange gases with the ambient environment. The packaging for the microsystem includes a flexible polyimide electronic ribbon cable and four fluidic ports that provide external interfaces to electrical energy, closed-loop sensing and electronic control as well as solid and liquid supplies. The complete structure has a size of $(2.5 \times 2.5 \times 0.6)$ cm^3. We have employed the device to successfully culture BHK-21 cells autonomously over a three day period in ambient environment.**

***Index Terms*—Cell culture, CMOS, poly(dimethylsiloxane) (PDMS), microfluidic, micro-incubator, 3-D microsystems.**

I. Microengineering for Cell Culture and Incubation

CELL-CULTURE techniques, developed at the turn of the 20th century, are still today the enabling and fundamental tool in the study of cell function, tissue engineering and pharmacology. From a scientific perspective, cell-culture studies have revolutionized our understanding of cellular and molecular biology and have been integral to the development of mass-production viral vaccines, *in vitro* fertilization, pharmaceutical screening, and toxicology. This has had a huge impact on public health and quality of life for the vast majority of the world. Furthermore, in the past 30 years, the development of artificial tissue and organs, cultured skins cells used today as grafts and wound dressings for burn victims and skin ulcer patients have been a direct result of basic research that relies on cell-culture techniques. Cell culture has also dramatically decreased the need for live-subject testing (both animal and human) and it is today the cornerstone of the world's fastest-growing industry, biotechnology [1].

However, for almost a century, traditional cell culture, plating cells in a standard vessel with a homogeneous substrate, media and reagents, has remained virtually unchanged with a limited variety of assays that could be performed. Recent developments in microfluidics have catalyzed the first steps toward a new methodology for cell culture. These advances are based on the adaptation of microfabrication techniques to biological applications, through soft lithography [2] and its application to microstructuring of soft polymer materials. More specifically, poly(dimethylsiloxane) (PDMS) has become the mainstay of soft lithography for applications in the life sciences. The low cost (approximately 50 times cheaper than silicon [3]), biocompatibility and its ability to be readily adapted to microfabrication techniques are among the numerous reasons PDMS has become immensely popular. A startup company focused on microreactors for high throughput protein crystallization [4] and a journal, *Lab on a Chip* [5], have emerged based on PDMS use in fabrication of microcomponents for applications in the life sciences. Numerous devices have been demonstrated using PDMS to create structures for cell growth [6]–[9].

There is a distinction between the fabrication of microelectronic devices and PDMS microfluidics that is important to address. Soft lithography requires the use of traditional microfabrication techniques simply to produce a master mold that is reusable, implying that access to expensive and sophisticated fabrication facilities is not needed in creating the devices, only master copies. The latter process translates the *per wafer* economic and environmental costs to a *per design* cost.

While there have been many recent developments in macroscopic [10], [11] and microfabricated structures for passive cell culture, in all but one of the published studies, a traditional incubator [12], [13] or complex fluidic heating and pumping system [8], [14] is employed for the actual cell culture. There has been only one published paper, that we are aware of, which attempts to integrate cell culture with "self incubation" in ambient environment. The cell-based biosensor (CBB), reported by Debusschere and Kovacs [15], includes all of the advantages previously described through the integration of a CMOS substrate with PDMS microfluidics for cell culture and biosensing. However, in this work the incubation feature was only used to maintain the cells during biosensing, periods between which the cells

Manuscript received January 4, 2007; revised January 15, 2007. This work was supported in part by the National Science Foundation under Grant ECS-0225489, "Cell Clinics On a Chip." The work of J. B. Christen was supported in part by a National Science Foundation Graduate Research Fellowship and a National Science Foundation G K-12 Fellowship. This paper was recommended by Editor-in-Chief T. S. Lande.

J. Blain Christen is with The Johns Hopkins School of Medicine, Johns Hopkins University, Baltimore, MD 21218 USA.

A. Andreou is with the Department of Electrical and Computer Engineering and the Whittaker Biomedical Engineering Institute, The Johns Hopkins University, Baltimore, MD 21218 USA (e-mail: andreou@jhu.edu).

Color versions of some are all figures are available online at http://ieeexplore.ieee.org.

Digital Object Identifier 10.1109/TBCAS.2007.893189

1932-4545/$25.00 © 2007 IEEE

were returned to a traditional incubator. In the published work [15], no details were given on the design of the PDMS structure and although their system does not eliminate the need for an incubator, the combination of CMOS and PDMS is unique and an important milestone in the field.

In this paper, we present a new paradigm for life sciences microsystem design and fabrication. The essence of the approach is the integration and embedding of CMOS electronics "into" PDMS microfluidics. We ground our work through a specific system central to life science research and biotechnologies: the cell incubator. We fabricate disposable microfluidic structures to control and manipulate liquids and gases that employ reusable functional CMOS silicon blocks integrated into the system. *Our approach is aimed at simple, inexpensive fabrication methods for components with elementary fluidic functions for use in tandem with very expensive, highly functional components that can be created once for reuse many times in the same or other systems.*

In Section II, we present the system architecture for a stand alone cell culture and incubation microsystem. The design of the microfluidic and CMOS electronic components of the micro-incubator are discussed in Sections III and IV, respectively. Section V outlines the thermal modeling for the culture well and the packaged microsystem as whole. The fabrication and integration of the PDMS components are described in Section VI. This is followed by the methods and results of experimental testing of the system's thermal characteristics in Section VII. Section VIII presents the cell-culture aspects of the work. We discuss the work presented in Section IX, and finally the conclusions are reported in Section X.

II. Micro-Incubator System Architecture

Standard incubators for cell culture provide an environment of 37 °C, 5% CO_2, and 100% relative humidity (RH). This temperature is the optimal growth temperature for most mammalian cells. The humidity is necessary to prevent the evaporation of water from the media, since this would affect the concentration. The CO_2 concentration is increased above atmospheric levels to maintain the proper pH, not for cell metabolism which requires atmospheric levels of both carbon dioxide and oxygen. During different phases of the cellular growth cycle the cells give off different amounts of CO_2 and lactic acid. During the "lag phase" the amount of CO_2 produced is not enough relative to the lactic acid to maintain physiological pH, 7.2–7.4. Each of these constrains must be met to provide a viable structure for incubation in atmospheric conditions. A typical research laboratory incubator is the size of a small refrigerator [see Fig. 1(a)].

In this section, we address each of the functional constraints in designing an autonomous cell-culture and incubation microsystem. We also discuss the methodology employed to define the necessary architecture, including the fabrication of the fluidic structures and the integration of the individual components into a microsystem at the chip-scale [see Fig. 4]. Our design overcomes the few remaining obstacles to achieving a completely portable, self-contained, low-cost cell-culture and incubation microdevice for use in the lab or in the field.

The micro-incubator system architecture is comprised of three main components [see Fig. 1(bottom)].

1) One or more hybrid microdevices depicted in Fig. 4 that includes disposable cell culture vessel, fluidics, fluidic ports and reusable CMOS microheater/solid-state temperature sensor.
2) An interface DAQ board that connects to a computer serial or USB port and incorporates a microcontroller, digital to analog converters to read out the temperature in the culture well as well as digital to analog converters to control the temperature in the device.
3) A computer for control and data acquisition. Closed-loop temperature regulation for each microdevice is accomplished through a proportional-derivative-integral (PID) controller in software.

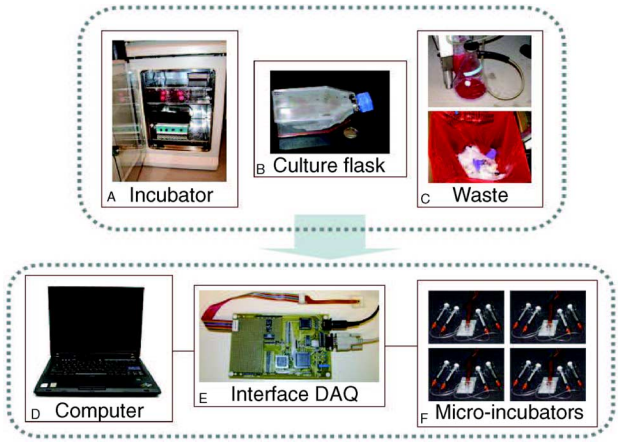

Fig. 1. Laboratory incubators have the size of a small refrigerator (a) and culture is done in palm-size flasks (b) or multiwell plates, that result in both materials and media waste (c). A micro-incubation system architecture involves one or more hybrid silicon CMOS/PDMS structures (f), an interface DAQ (e), and a computer (d) that controls the environment in each cell culture microdevice.

A. Interface DAQ

The DAQ interface is comprised of a custom PCB, a PIC microcontroller (PIC18LF6680, Microchip Technologies, Chandler, Arizona), two CPLDs, and an RS-232 interface. The PIC was programmed to communicate with its onboard ADCs and an onboard LTC1660 DAC. The DAQ was controlled via MATLAB files that provided ADC and DAC functionality for testing and operation of the hybrid microdevice.

The heater control circuit was designed to take a voltage input in the range of 0–5 V at a high impedance node and set the current of the on-chip heater. This is accomplished through an LF356 JFET input operational amplifier with feedback through a BS170P n-channel enhancement mode vertical DMOS-FET as shown in Fig. 2. The circuit works by setting the input V_{in} from the DAQ at the noninverting input node of the amplifier. The negative feedback combination of the DMOS FET with the operational amplifier, together with the 800 Ω resistor at the source of the DMOS-FET set the current, I_{out} in the heater.

B. PID Temperature Control

A diode-based proportional-to-absolute temperature (PTAT) thermometer circuit is implemented to monitor the temperature at the surface of the cell-culture vessel (CMOS die). The differential voltage output of the circuit is measured using an INA101 instrumentation amplifier with a single resistor G to control the gain set to approximately 40. The voltage is digitized using an ADC converter and read by the software on the computer to close the control loop.

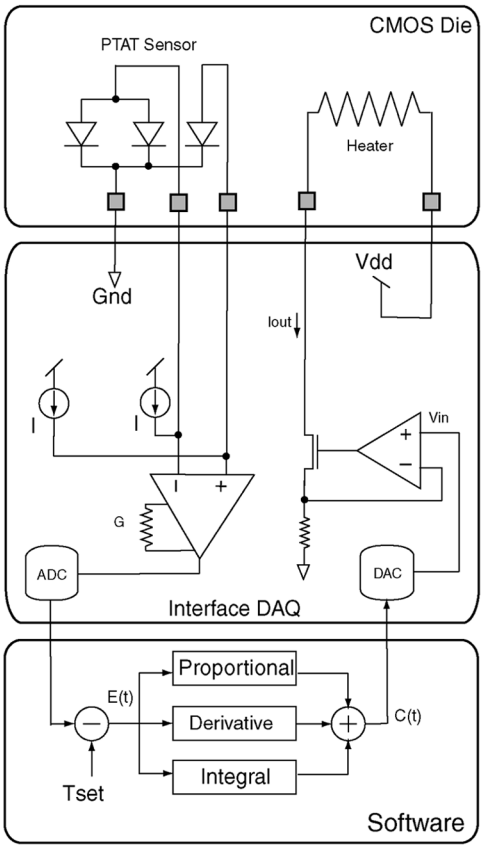

Fig. 2. Microelectronics system architecture of the cell culture and incubation microdevice. It is comprised of three components (i) a CMOS die, (ii) an interface DAQ, and (iii) software for closed loop control and data acquisition.

While many different control system algorithms or control loops exist (e.g., bang–bang or "on/off," linear or fractional order control), it is important to chose one well suited to the application and system requirements. PID controllers have been long known for being effective in control and regulation of thermal systems. Each of the terms, "proportional," "integral," and "derivative" refers to one of the three basic elements of a PID controller. Each of these elements performs a different task and has a different effect on the function of a system. The general form of a PID controller is shown in Fig. 2. The system can be described mathematically through (1) where $E(t)$ is the error, K_P, K_I, and K_D are the proportional, integral, and derivative constants, respectively, and $C(t)$ is the control output of the system

$$C(t) = K_P \times E(t) + K_I \int_0^t E(t)dt + K_D \frac{dE(t)}{dt}. \quad (1)$$

Intuitively, the PID controller can be thought of as attempting to control temperature at some value T_{set} by looking at the current error, past error and predicting future error. The proportional control handles current error by quickly responding with large changes in the output. The integral control looks at past error, keeping a running total of the past error and changing the system until this total is zero. The derivative control predicts the future by looking at the slope of the error. This slope gives information on the rate of temperature change.

As shown in (1), the formula for calculating the input to the system is a continuous function. Since most modern control systems (including the DAQ employed here) operate in discrete time, it is necessary to convert the continuous function into discrete-time function. This transformation requires approximations for both the integral and derivative portions of the equation to obtain the discrete-time PID formula as shown below where t_S is the sample period. We use a simple first-order approximation to the derivative to derive

$$K_P E(t) = K_P E(n)$$
$$dE(t)/dt \cong [E(n) - E(n-1)]/t_S$$
$$\int_0^t E(t)dt \cong t_S \sum_0^n E(n)$$
$$C(n) \cong K_P E(n) + [E(n) - E(n-1)]/t_S + t_S \sum_0^n E(n).$$

The final step in implementing the system is choosing the constants or "loop tuning." For PID control, this is a fairly simple process since the system will operate efficiently even if the constants are not very well tuned. The basic method for tuning is to set all of the constants to zero and increase the proportional constant until it begins to oscillate or overshoot by more than 50%. Once the system is oscillating, the derivative constant is increased until the overshoot is eliminated. Finally, the integral constant is increased until the system operates within acceptable parameters [16], [17]. Using this methodology we the following constants are obtained for the system described in this paper, K_P=1.3, $K_I = 0.1$, and $K_D = 0.01$.

While PID control is a powerful method of temperature regulation, it is susceptible to noise. If the disturbances in the system are significant, the derivative term will cause large fluctuations in the output unnecessarily. Thus, in the system discussed here, the derivative constant is very small compared to the other constants.

C. Packaging and Interfaces

Packaging for hybrid systems that incorporate microelectronic, microelectromechanical systems (MEMS), and microfluidic components presents several challenges unique to a system that operates in different domains. Packaging for hybrid systems must take into consideration not only the needs of each component of the system, but the interactions between the components. When integrating fluidic with electronic components, the interconnects for the semiconductor component(s) must be modified to enable function in an aqueous environment, requiring a barrier between the electronics and solution (media). This passivation must, in addition to providing electrical insulation, provide physical protection to the bonding wires. In the case of the chip scale incubator discussed here, ideally the temperature of the culture vessel should be controlled solely by the on-chip devices. In practice, this is not the case due to the effects of the environment and hence an additional role for packaging is to isolate the cell culture and incubation area from environmental effects as much as possible. Although every interface to the chip acts as a heat sink or source, high thermal conductance paths to the environment should be minimized to decrease the power necessary to maintain the desired temperature in the culture well.

The microsystem presented in this paper necessitates two or more different types of interface, microelectronic and microfluidic. If these interfaces are not implemented in a proper manner the system will become physically unstable, awkward and difficult to use. The planar profile of the electronics packaging is important for hybrid microfluidic systems. Microfluidic layers fab-

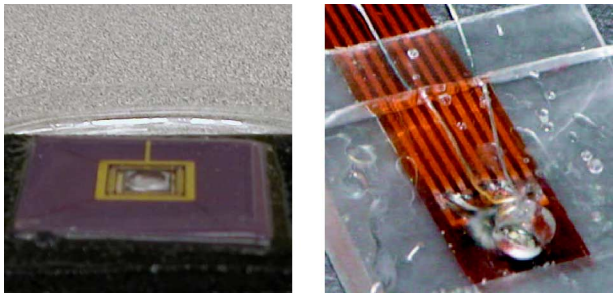

Fig. 3. Silicone fluidic structure ON packaged silicon (left) and packaged silicon IN silicone (right).

ricated using the soft lithography techniques that will be further discussed in the following sections are able to conform to surfaces with profile changes only if they are gradual. While it may be possible to use dielectric materials to change the planar profile of packages, this creates a gap between the surface of the chip and the microfluidic components. Such a gap prevents the fluidic channels from flowing directly over the surface of the chip hindering functionality of the microfluidics and leading to structures limited to a "micro petri dish" configuration as shown in Fig. 3.

A packaging solution that eliminates the problems outlined above, while at the same time providing robust electronic interface to the microsystem employs a polyimide ribbon cable. Polyimide ribbon cables are used in flexible circuit technology and very commonly used for laptop displays. This type of interconnect is much more thermally insulating than standard CMOS packages and offers a very small, low profile interface ideal for integration. Waterproof adhesive with low viscosity was employed to create a conformal coating for the bond wires. The adhesive protected the bond wires during fabrication and provided both electrical and thermal insulation. Physical protection is especially important since the adhesive encapsulated bond wires exist at the interface between a rigid substrate (the silicon die) and the flexible microfluidic component; if the bond wires encounter physical stress, they can easily break causing the system to fail. In addition, a hole was cut into the area of the ribbon cable for chip placement, such that the chip did not physically contact the ribbon cable. The chip was secured to the ribbon cable using the same adhesive prior to wire bonding.

III. Analysis and Design of PDMS Fluidic Structures

The flow of liquids in the system is gravity driven. The analysis and design of the various fluidic structures under such *quasi-static* conditions can be done using simple calculations based on prior experience with PDMS fluidic channels.

A *multilayer* PDMS architecture (see Fig. 4) is employed to meet a multitude of design constraints and solve many of the most common problems encountered during cell culture and long term incubation in PDMS. The structures that have been reported in the literature thus far have had fluidic channels on a single level with cells cultured either in channels or with the channels and cell culture area having the same substrate. The advantages offered by the system architecture presented in this paper yield a system that is simple to fabricate, robust and highly functional tool for research and commercial applications. The following is a list of the three main fluidic design areas:

1) cell culture vessel;
2) fluidic channels;
3) fluidic ports and structural support.

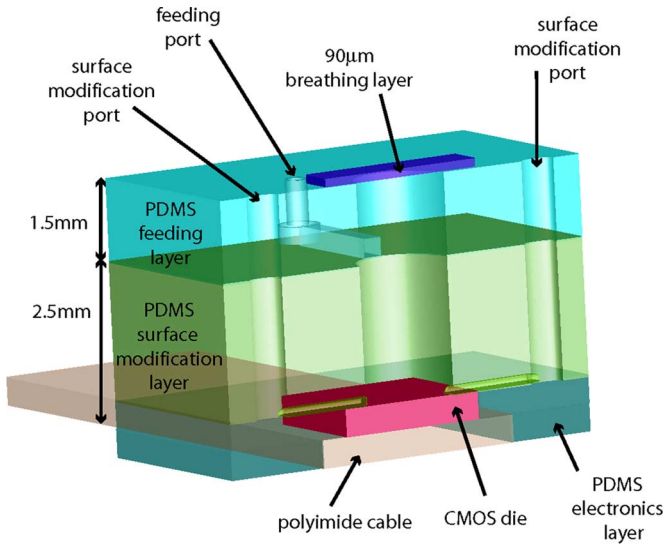

Fig. 4. Chip-scale incubator rendered in cross-sectional perspective. The layers from bottom to top are electronics encapsulation (including polyimide substrate and CMOS die), surface modification, feeding, and breathing layers.

A. Cell-Culture Vessel

The first design consideration for the micro-incubator system is creating an on-chip cell-culture vessel. In the passive PDMS, microfluidic devices that are currently used in research, cells are cultured in an environment that is quite different from the traditional cell-culture vessels. Aside from materials differences, the other important difference is in the geometry of the culture region. The height of the vessel can affect cell growth if the height is on the order of the height of the cells, as is the case in the designs that have been described in published work [8], [9], [14]. In addition, the amount of media used per surface area is much less than in traditional culture vessels. This necessitates media exchanged often to provide sufficient nutrients to the cells. This media exchange is the biggest source of sheer stress in other systems and requires more complex feeding systems. Moreover, the amount of media provided as well as the height of the media above the cell-culture substrate are extremely important to cell growth. If the volume is too low, the media will become deplete such that adequate nutrients are no longer available to the cells. However, if the initial volume of medium is too great or the media replenished is too rapid (as is often the case in published work), cells will be unable to condition their environment adequately. The recommended volume of medium for routine substrate-dependent culture is 0.2–0.3 mL/cm^2. Since the medium overlying the cells acts as a barrier to gas diffusion, not only the total volume, but the height of the media above the culture substrate is important in allowing sufficient diffusion of CO_2 and O_2.

The microsystem presented in this paper, unlike other systems published to date, is a scaled down model of the traditional vessels used for cell culture. As shown in Table I, the geometry of the culture vessel is such that ϑ is matched to the media depth and volume for traditional cell culture. The height was controlled by creating a surface modification layer (see Section III-B) with height equal to the desired media depth. By elevating the entry and exit ports for media exchange, the well fills

TABLE I
CELL-CULTURE VESSEL GEOMETRY—MACROSCALE AND MICROSCALE CELL-CULTURE VESSEL GEOMETRY. AREA IS THE ACTIVE CELL CULTURE FOR THE DEVICE. DEPTH IS THE MEDIA AND/OR CHANNEL DEPTH AND ϑ IS THE RATIO OF THE MEDIA VOLUME TO THE ACTIVE CELL-CULTURE AREA. ϑ DIFFERS FROM THE CHANNEL OR MEDIA DEPTH ONLY WHEN THE SURFACE AREA OF THE DEVICE AND THE ACTIVE CELL-CULTURE AREA ARE NOT EQUAL. THIS VALUE IS INDICATIVE OF THE AMOUNT OF MEDIA PER CELL. VALUES FOR THE STANDARD CULTURE VESSELS WERE TAKEN FROM [1] AND THE VALUES FOR THE PDMS STRUCTURES WERE DERIVED FROM REPORTED GEOMETRIES [12]–[14]

Vessel	Area (cm^2)	Depth (mm)	ϑ (mm)
Flasks			
	25	2.4	2.40
	75	2	2
	150	2-2.67	2-2.67
	162	2.78	2.78
Multi-well plates			
6-well	9.5	2.1	2.1
12-well	4	2.5	2.5
24-well	2	2.5	2.5
48-well	1	2.5	2.5
96-well	0.32	3.13	3.13
PDMS Cell Culture Devices			
This work	0.0177	2.5-3	2.5-3
Folch et. al	0.0085	0.25	5.1
Leclerc et. al	1	0.027	0.27
Lee et. al	0.0079	0.004	0.04
Vacanti et. al	6.09	0.035	0.035

to this height before excess media exits through the channel on the opposite side of the well. Creating a structure matched to traditional culture vessel geometry eliminates the need for an automated perfusion system and allows for transfer of experiments onto a microfluidic platform without the modifications to protocol and chemistry.

In designing a truly autonomous micro-incubator system that operates in ambient environment, the decision is made to design the system for CO_2 independent cell growth. CO_2 independent media uses Hank's balanced salt solution or Dulbecco's phosphate-buffered saline to maintain the proper pH within the culture at an atmospheric CO_2 level. This is in contrast to CO_2 dependent media containing Earle's balanced salt solution or Eagle's spinner salt solution both utilizing sodium bicarbonate to buffer the pH, but requiring additional CO_2 from another source, namely the incubator as previously stated. It should be noted that the use of media with Hepes buffer, commonly used in PDMS cell-culture devices, is not sufficient for CO_2 independent cell growth. The presence of Hepes buffer acts to slow the change in the pH of the media but does not prevent variation in the pH. Through the change in media buffing system, the need for an elevated level of CO_2 via an extrenal carbon dioxed supply is eliminated.

To maintain the proper media concentration and provide for the exchange of both carbon dioxide and oxygen with the environment, a breathing layer is incorporated into the design. This layer caps the cell-culture vessel with a thin, 90-μm layer of PDMS. The breathing layer is hydrophobic, limiting the outward flow of water vapor, and gas-permeable to maintain proper O_2 and CO_2 levels in the cell-culture vessel.

The thickness of the breathing layer must be such that it allows gas exchange with the environment at a rate sufficient to sustain cell growth. An upper bound on the appropriate thickness for this membrane can be calculated from the geometry of the micro-incubator, physical properties of PDMS and the oxygen consumption.

The O_2 consumption for a confluent monolayer of cells is $1.00 \times 10^{-16}(\text{mol})/(\text{cell} \times \text{s})$ [18]. Given a confluent cell density of 4.00×10^6 cells/cm^2, this results in O_2 consumption of $4.00 \times 10^{-10}(\text{mol})/(\text{cm}^2 \times \text{s})$.

The oxygen flux for the device is given by the product of the diffusivity of oxygen through PDMS D_{PDMS} and the concentration gradient ΔC divided by the thickness of the membrane t

$$F_{\max} = \frac{D_{\text{PDMS}} \times \Delta C}{t}.$$

The diffusivity oxygen through PDMS is 18×10^{-6} cm^2/s [19] and the concentration gradient for oxygen is 2×10^{-7} mol/cm^3 [8]. Thus, the diffusion of oxygen through PDMS is $36 \times 10^{-13}(\text{mol})/(\text{cm} \times \text{s})$. To obtain sufficient oxygen diffusion through PDMS the thickness of the membrane must allow a flux that is no less than the oxygen consumption, so by equating these values we can obtain an upper bound on the thickness.

$$O_2\text{consumption} = \frac{D_{\text{PDMS}} \times \Delta C}{t}$$

$$4.00 \times 10^{-10} \frac{\text{mol}}{\text{cm}^2 \times \text{s}} = \frac{36 \times 10^{-13} \frac{\text{mol}}{\text{cm} \times \text{s}}}{t}$$

$$t = 9 \times 10^{-3}\text{cm} = 90\ \mu\text{m}.$$

Thus to maintain the necessary oxygen level for a confluent monolayer of cells, the barrier between the cells and the oxygen in the ambient environment (air) must be no more than 90 μm.

B. Fluidic Channels

The cell-culture microsystem includes two sets of channels of different geometry. These channels are the adhesion factor channels in the surface modification layer and the feeding channels in the feeding layer.

The adhesion factor channels have a height of 11 μm and base width of 20 μm with a semicircular cross section and directly interface the cell-culture substrate, being formed directly atop the CMOS die. This geometry ensures that the adhesion factor will fill the well during application to a height of 11 μm, approximately the maximum height of a cell during all growth phases. The result is that the only surfaces coated and modified are the base and a small portion of the sidewalls. This guarantees that the only surface in the structure to which the cells adhere is the base of the well. Coating a small portion of the sidewalls ensures that cells will proliferate along the perimeter, since the adhesion factor not only allows cells to attach to the surface, but also increases the hydrophilicity of the surface. It is also important to limit the height of the adhesion factor to that of a single cell to prevent cells from adhering to the sidewalls and proliferating up the sides to cover an area greater than the base. Finally, limiting the height of this channel helps to prevent cells from proliferating from the well into the channels. It is important that the cells are grown only on the heated surface.

The feeding channels are formed atop the surface modification layer in the feeding layer. The channels have a rectangular cross section with a height of approximately 150 μm and width of either

200 or 500 μm (both sizes were successfully employed). These channels serve three purposes: plating, feeding, and subculturing. First, they are used to plate the cells in the well. Since the plating and surface modification are performed in separate channels, the adhesion factor never enters these channels. Thus, the cells will not adhere to the surfaces of the channels. This means that cells are easily removed from these channels after seeding by flushing with media. In both sets of channels, it is important that the cells are not allowed to remain within since the architecture depends on cell presence exclusively at the base of the well. To ensure that dead cells are not present in the system during culture, they are plated, allowed to adhere (approximately 1–2 h); then the channels are flushed with media removing any cells that have not adhered to the substrate. This is beneficial not only in removing cells from the channels, but it is also a "Darwinian" selection method for cells that were initially present in the well. Any cells that were not healthy enough to adhere to the substrate during this period will be flushed away leaving only healthy cells in the on-chip vessel for culture.

The feeding channels are also used to renew the media or "feed" the cells. The larger cross-sectional area of these channels not only allows cells pass through easily for plating/seeding but also require very little pressure to create flow for feeding. The reduction of pressure is beneficial for cell growth since media flow is one of the most common reasons for impaired cellular growth in microfluidic cell-culture devices. Even more importantly, the feeding channels exist several millimeters above the culture substrate. This means that the direction of media flow is perpendicular to the substrate rather than in-plane. The change in the direction of media flow is particularly important for cell-culture devices since cells are much more susceptible to shear stress than direct stress [20]. While many reported devices use complex in-plane structures to reduce shear stress, this is the only device reported to date that uses a multilayer architecture to completely eliminate shear stress.

Finally, the channels in the feeding layer are used for on-chip subculture allowing for the introduction of trypsin to the culture area. Trypsin is used in traditional culture to remove all cells from a culture substrate, however, it can also be used to remove a portion of the cells by limiting the exposure time. A limited exposure to trypsin will result in a reduction of the number of cells attached to the substrate. Any cells that are either dead or no longer attached to the substrate will float to the top of the on-chip vessel, along the plane of the feeding channels. These cells are easily flushed out of the culture area with media through the same channels. The introduction of media during this process with not only serve to remove the unwanted cells, but also to neutralize the trypsin and replenish the well with fresh media. The remaining cells will begin to proliferate (divide) once again due to the reduction in cell density. We have successfully performed three consecutive subcultures in the microfluidic structure presented in this paper.

C. Fluidic Ports and Structural Support

In PDMS microfluidics devices, the total thickness of the input and interconnect layers (height of the PDMS above the channel) must be sufficient to support the needle or hypodermic tubing in the ports, approximately 1.5 mm or more for 23 gauge. If the ports are not properly supported the hypodermic tubing will deform the PDMS port causing it to leak or tear. Damage to the ports was the most common structural failure mechanism.

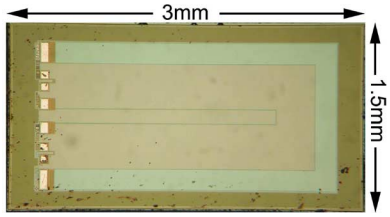

Fig. 5. Microphotograph of the second generation thermal control chip. The large partial loop structure along the perimeter of the chip is the polysilicon heater. A second loop structure in the middle of the chip, is a polysilicon wire that can be used as second heater to create thermal gradients on the chip.

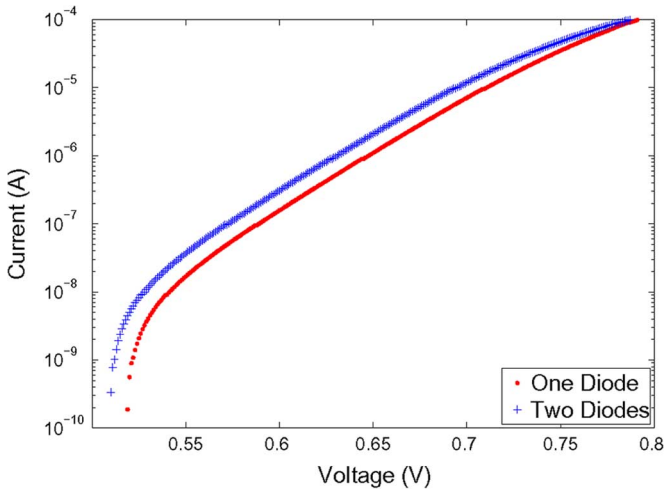

Fig. 6. Current as a function of the applied voltage for the diodes in the PTAT circuit at room temperature (approximately 300 K). The diodes exhibit a region where the current has an exponential dependence on the applied voltage at an optimum bias point of approximately 0.6 V.

IV. Analysis and Design of CMOS Electronics

A CMOS integrated circuit was designed to integrate the heater and the temperature measurement sensor. The first generation of the silicon chip used polysilicon wires as the heater and the temperature sensor [21]. However, the need for individual device calibration lead to an alternative design in this paper that employs a calibration-free PTAT temperature sensor.

A. Polysilicon Heater and PTAT Temperature Sensor

A PTAT circuit shown in Fig. 7 was implemented to give a calibration-free accurate measure of the temperature. The chip has dimensions of 3×1.5 mm^2 and was fabricated in a 1.6-μm single polysilicon layer, two metal layers CMOS technology (see Fig. 5). The heater was composed of a partial loop of polysilicon. The width of the heater was 210 μm and the length was 6780μm. The total resistance of the heater including the bonding wires was approximately 800 Ω. The PTAT circuit implemented on this chip was a three-diode design. The diodes were created using the junction between n-diffusion in an n-well and p-diffusion. The length of the junction was 9.6 μm. Each of the three diodes has the same geometry and orientation with two connected in parallel and the third independent of the other two. Characterization of the single diode and diode pair is shown in Fig. 6.

The basic equation for the current I in a forward-biased diode is given by

$$I = I_S e^{\frac{V_d}{nV_t}}$$

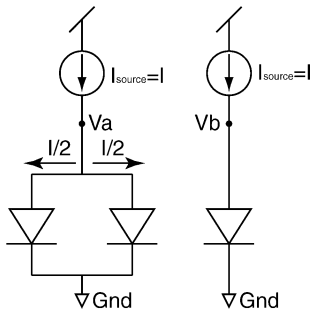

Fig. 7. PTAT circuit.

where I_S is the saturation current, V_d is the applied voltage, V_t is the thermal voltage given by

$$V_t = \frac{kT}{q}$$

where k (Boltzman's constant) is 8.617 eV/K, T is the temperature in kelvin, and q is the magnitude of electronic charge, 1.602×10^{-19}C. The constant n depends on the material and physical structure of the diode and in the ideal case it is equal to 1.

If the diode equation is put in terms of the voltage drop across the diode

$$V_d = \frac{1}{n}\frac{kT}{q}\ln\frac{I}{I_S}.$$

The PTAT circuit gives a differential voltage output $V_A - V_B$ that is independent of the current and proportional to the absolute temperature. Given that the two diodes in parallel are of equal geometry, the current through each of the diodes will be one half the total current. Thus, we can represent the equations for the voltages V_A and V_B with

$$V_A = \frac{kT}{nq}\ln\left(\frac{\frac{1}{2}I}{I_S}\right)$$
$$V_B = \frac{kT}{nq}\ln\left(\frac{I}{I_S}\right).$$

The difference between the two voltages is given below. Using the subtraction/division identity for natural logarithms, $\ln X - Y = \ln(X/Y)$, we can simplify the equation

$$V_B - V_A = \frac{kT}{nq}\ln\left(\frac{I}{I_S}\right) - \frac{kT}{nq}\ln\left(\frac{\frac{1}{2}I}{I_S}\right)$$
$$V_B - V_A = \frac{kT}{nq}\ln(2).$$

Thus an expression for the voltage difference between the two nodes, V_A and V_B, shown in Fig. 7 can be derived in terms of a single variable T. Characterization of the circuit is shown in Fig. 8.

V. Finite-Element Thermal Analysis

The design of a chip-scale thermal microsystem necessitates a good understanding of the system's thermal behavior; in particular, the mechanisms responsible for heat losses to the ambient environment. The complex geometries and hybrid structure as well as the small scale and associate small thermal mass of fluids involved, necessitate the use of numerical finite element analysis methods to validate rough design calculations. While it is not practical to empirically test a wide variety of proposed designs, it is feasible to perform finite element analysis on each design to compare their relative performance. The use of such tools together with experimental testing allows for exploration of the microsystem architectural space.

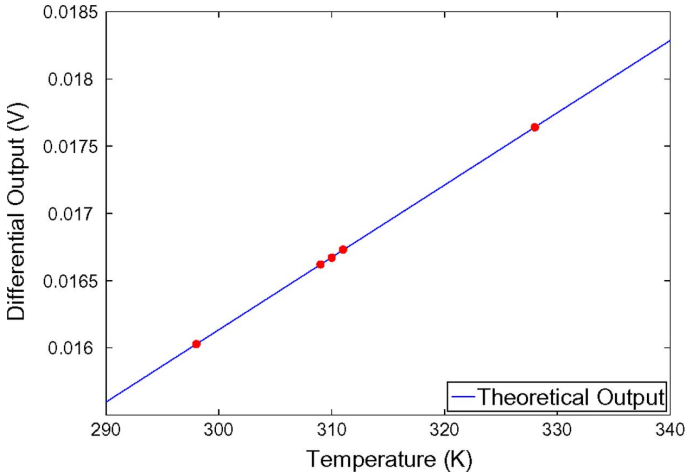

Fig. 8. Experimental characterization of the PTAT circuit. The voltage outputs from the chip tested in a thermal chamber are plotted (filled circles); a theoretical curve calculated from the PTAT equations shows excellent match to the experimental data.

In the following analysis, we used Comsol Multiphysics [22] with Electromagnetics and Heat Transfer and modules. The material properties were obtained from the sources as indicated in Tables IV–VI of Appendix A.

A. Thermal Analysis of the Culture Vessel

The results from the model for the heater chip were used to simulate the thermal properties of the micro-incubator. Simulations were performed with different amounts of fluid, 500 μm, 2 mm, and 4 mm (filled), to ensure that evaporation would not significantly affect the temperature along the surface of the chip where the cells would be located. The composite convection and conduction problem was solved via (2), where V is the voltage, k is the thermal conductivity, T is temperature, Q is the heat source, ρ is density,C_ρ is heat capacity and u is directional velocity

$$\nabla\cdot(-k\nabla T) = Q - \rho C_\rho u\cdot\nabla T. \quad (2)$$

The results of the simulation showed that the temperature within 10 μm of the surface of the chip (where the cells would be located) varied by no more than 0.005° with respect to the amount of fluid in the well. The temperature variations throughout the depth of the well and with emphasis on the fluid near the surface are shown for the worst-case scenario (500 μm of fluid) in Fig. 9.

B. Thermal Analysis of Packaged Microsystem

We have also used finite element analysis to compare the heat flux necessary to maintain the cell-culture area at 37 °C for a polyimide ribbon cable and a ceramic DIP28 (based on schematics provided by Kyocera Inc., Kyoto, Japan). The open cavity ceramic DIP28 is a standard package offered through chip prototyping services, such as MOSIS and EuroPractice. These packages are, in fact, designed to act as heat sinks, since traditionally heat generated by circuits is an unwanted side-effect

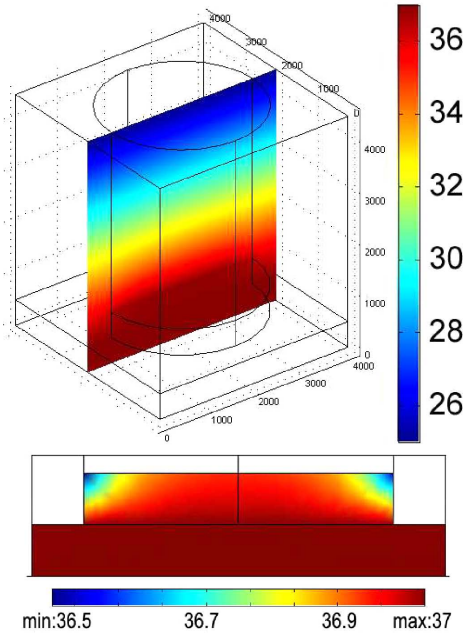

Fig. 9. Temperature in degrees Celsius (°C) within the well throughout the structure (top) and with emphasis on the fluid within 500 μm of the surface (bottom).

rather than a desired output. The results show a drastic difference in the heat flux necessary to maintain the thermal gradient between the chip and the environment. In solving for the power dissipation necessary to enable the DIP to maintain the temperature necessary for cell incubation, we found that it was must larger than can be generated nondestructively with a CMOS die; almost three orders of magnitude more than the ribbon cable!

The results for the ribbon cable packaging showed a much more reasonable value for the heat flux necessary to maintain this temperature and compares quite well to experimental results (see Section VII). The 2-D finite element analysis results showed a heat flux of 7.029×10^{-8} W/m^2 generated by resistive heating was sufficient to maintain the proper temperature for the incubation environment, while the DIP required $1.80 \times 10 - 5$ W/m^2 be provided by the heater. The temperature profiles for the DIP and ribbon cable packaging with this heat flux are shown in Fig. 10.

VI. PDMS Components Fabrication and Integration

In this section we discuss the basic step followed to fabricate the PDMS fluidic structures. Photolithography was performed on 3-in silicon wafers with standard techniques and developers, unless indicated. The masks for the photolithography were 5000 dpi transparencies printed by PageWorks [23]. The resolution of the masks was 5 μm and the minimum feature that could reliably be patterned using these masks was 15 μm. A Quintel Expo Model 7K8 mask aligner was used in the photolithography. We used Shipley S1813, SJR 5740 and SU8-2100 photoresists to create patterns with thicknesses of 0.5–1, 11, and 150 μm, respectively.

A. Master Mold Fabrication

We fabricated three types of master molds: blank (breathing layer), positive (surface modification layer, 11 μm), and negative (feeding layer, 150 μm). There were two exceptions to the

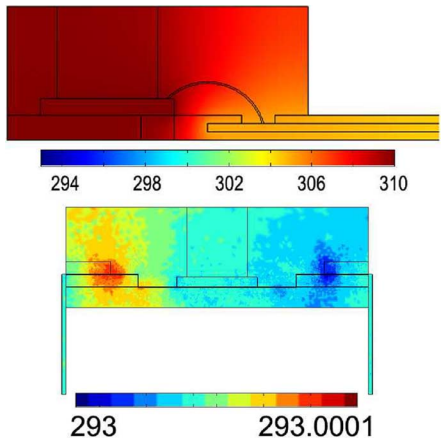

Fig. 10. Temperature plot in Kelvin (K) for polyimide ribbon cable near the micro-incubator (top) and ceramic DIP (bottom) with equivalent heating.

standard protocols for creating these molds. First, in each case the fabrication started with creating a thin layer of unpatterned photoresist on top of the silicon wafer that was hard baked at 200 °C overnight. For the blank master mold, no additional processing was performed. The other two molds were created by patterning the appropriate photoresist on top of this layer. While this step is trivial to carry out, it eliminated the need for a release agent and/or plasma etching. Second, we used reflow on the surface modification layer to increase the yield.

B. Replica Molding

We used standard replica molding techniques to fabricate the microfluidic components (see Fig. 11). Throughout this work, General Electric RTV 615 (mixed in a 10 A to 1 B ratio by weight) was used and cured in a Blue-M oven. The three master molds described above were used to create layers with different thicknesses. The surface modification and feeding layers had a thickness of 2.5–3.0 and 1.5–2.0 mm, respectively, and were fabricated by casting. The blank molds were used to create a 90-μm-thick layer of PDMS for the breathing layer by spinning the PDMS pre-polymer onto the blank mold.

C. Embedding CMOS Electronics in Multilayer PDMS Structures

Another of the advantages of using PDMS is the simplicity with which additional devices can be added to the structure by embedding to create heterogeneous 3-D structures. In fabrication of the PDMS layers, devices can be embedded during replica molding. There are two methods that can be used to achieve this effect, interfacial or noninterfacial embedding. For interfacial embedding, the device to be embedded is placed on the master prior to casting PDMS. This procedure will embed the device at the interface of the layer created by the master mold and the layer below. The other method, noninterfacial, is used to embed the device totally within a single layer. This can be accomplished by pouring a portion of the PDMS over the master, partially curing (leaving the surface very tacky), then placing the device on the partially cured PDMS. The remainder of the PDMS is added to the container until the device is covered and the desired layer thickness is obtained. The device must be covered so that layers assembled above will properly conform to the surface. We used the noninterfacial embedding technique

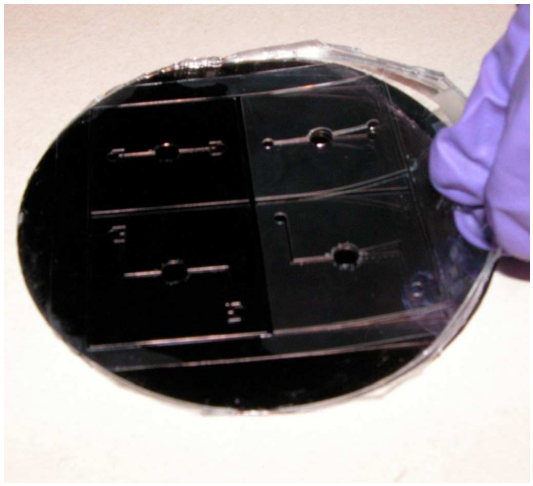

Fig. 11. Cured PDMS created using standard replica molding techniques peeling away from a master mold. The feeding layer is shown.

to embed a type J IRCO-010 [24] thermocouple in the surface modification layer to independently measure the temperature of the well (see Fig. 3). Once the thermocouple was embedded the surface modification layer was cured in the same manner as a master mold without a thermocouple.

The CMOS die was received unpackaged from the foundry. The dies were cleaned with ethanol followed by deionized water by repeatedly soaking, rinsing and gentle wiping with cotton-free, woven polymer wrapped foam tipped swabs (Techni-Tool). This procedure is necessary, because unlike custom fabricated structures, that are prepared in a laboratory under well controlled conditions, foundries use dicing processes that may leave residue on the surface that poisons cells.

The cleaned die was wire-bonded to a flexible polyimide coated substrate. The wire bonds were covered with a small amount of Loctite adhesive sealant to protect the wire bonds. The adhesive was cured with UV light at a dose of 800 mW/cm^2. This step is necessary since the wire bonds are very delicate, and if PDMS is used to cover the bonds, its deformation during fabrication and use will most likely cause the bonds to break. After curing, the adhesive was cleaned and covered by a very thin layer of PDMS.

The final step in preparing the electronics was to create a level substrate using PDMS. The ribbon cable was secured in a plastic petri dish with the passivated side of the CMOS die facing up, silicon substrate side down. PDMS was added to cover the assembly and lightly cured. After curing, the electronics layer was removed from the petri dish and turned over. This ensures a very uniform surface for the following steps. The layers assembled as described above were then placed on the side of the electronics layer that was in contact with the petri dish with the well structure directly above the back side of the CMOS die. A final curing step was performed on the complete microsystem overnight to ensure that the PDMS was fully cured and would not poison the cells. The completed micro-incubator can be autoclaved for sterilization.

D. Trimming and Punching Fluidic Ports and Wells

Each of the patterns on the master molds consisted of four tiled designs with an area of 2.5 $\times$ 2.5 cm^2. Each design was surrounded by scribe lines to imprint trimming guides into the PDMS. The ports, wells and interconnects were formed using a punch method. We used 1.5-mm-diameter biopsy punch to cut the large wells; this was the area defined for cell growth. The ports were formed using 23-gauge blunt end needles (stainless steel hypodermic needle with luer hub—blunt, NE-231PL [25]). The area patterned for the ports had approximately twice the diameter of the needle to eliminate any difficulty with alignment.

It is important that the well and ports were punched in the layers and assembled in the correct order to ensure self-alignment of interconnects and that ports do not extend below the channel they access. The first layer punched was the feeding layer containing the upper level channels. Then, its companion surface modification layer well only was punched. The wells of the two layers were then aligned and assembled. The alignment is extremely unimportant to the functionality of the CMOS incubator. The device needs only a small area of overlap between the wells, so alignment can be off by several millimeters and the device will be functional! Misalignment can however make it more difficult to image the cells, but all of the alignment for this work was done by hand with no magnification. Once the two layers were aligned and sealed (approximately 15 min at 55 °C). The ports for the surface modification layer were then punched through the entire structure to assure self-alignment.

Finally, the breathing layer was assembled above the well. The thin PDMS spun onto the blank master was trimmed cover the area of the well but not block any of the ports. The distance between the well and ports was designed to accommodate large variations in the size of the breathing layer. Then, a final "index-matching" step was performed by applying a very small amount of PDMS pre-polymer to the sides of the device perpendicular to the substrate. This step is optional makes the microfluidics transparent when viewed from the side.

The complete microdevice is shown in Fig. 12. We used 23-gauge blunt 1/2 inch needle (stainless steel hypodermic needle with luer hub—blunt, NE-231PL [25]), flexible tubing (polyvinylchloride tubing, Micro-Bore, TGY-020) and 23-gauge hypodermic tubing (stainless steel hypodermic tubing type 304, HTX-23R [25]) to create an interface between the micro-incubator and standard luer-lock syringes. This allows for easy exchange of luer-lock syringes to inject any fluid (or gas) into the PDMS channels and well.

VII. Thermal Characterization

The thermal characteristics of the system were studied experimentally in addition to the finite element analysis described in Section V. Experimental investigation of a system is important in confirming analytical results and detecting environmental variants that may not have been considered in determining the parameters for the computational analysis. The empirical investigation of the system also provided a measure of the different disturbance sources and their magnitudes, e.g., variations in ambient temperature.

The heater chip was tested with a PDMS well on both the front and back side to map the temperature within the well. The thermal characterization was performed using a micromanipulator xyz stage with a small gauge thermocouple mounted to the platform. The thermocouple mounted on the micromanipulator was used to sample the temperature in the reservoir. The thermocouple output was measured using a USB-TEMP

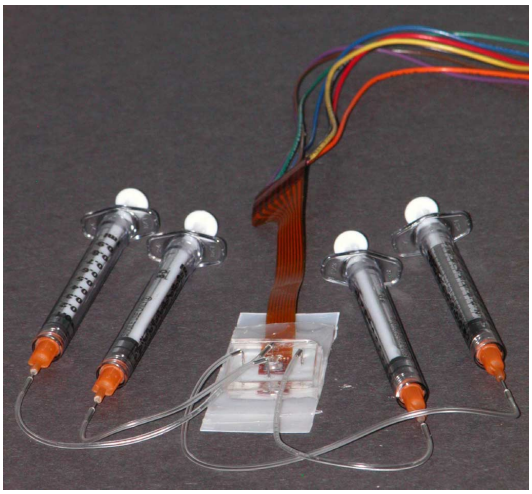

Fig. 12. Photograph of the assembled microsystem including fluidic and electrical interfaces. The breathing layer was removed for photography.

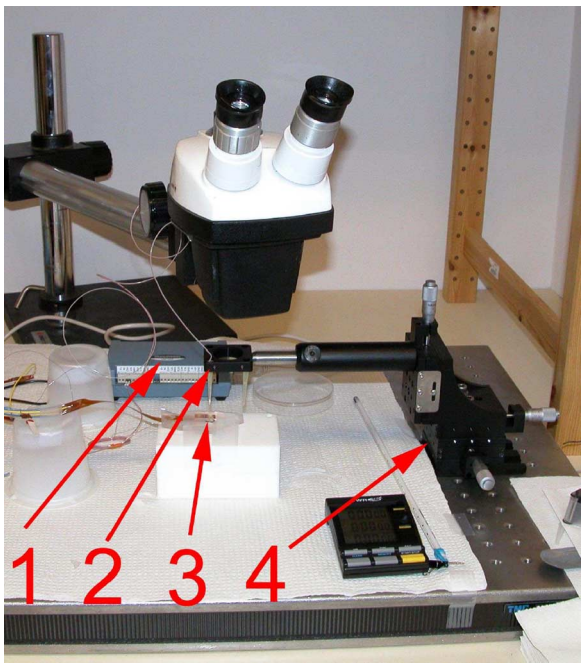

Fig. 13. Experimental setup for characterization of temperature within the micro-incubator. The setup includes a small gauge thermocouple (2) mounted on an xyz stage micromanipulator (4). The output of the thermocouple was measured using a USB-TEMP module with cold-junction compensation (1). The micro-incubator test structure (3) is shown mounted below the thermocouple.

module (Measurement Computing, Norton, MA). The measurements provided a 3-D profile of the thermal characteristics of the system. A second thermocouple was simultaneously used to monitor the temperature of the ambient environments. The measurement setup is shown in Fig. 13. The thermal characterization of the heater chip was performed for planes parallel to the surface of the chip through the height of the well. Measurements were taken at the surface of the chip and in 10-μm increments up to 100 μm above the surface. The measurements for both sides of the chip showed large variations. This variation is much larger than the two degree maximum that is required for viable cell culture [1]. However, raw measurement of the temperature does not account for fluctuations in ambient

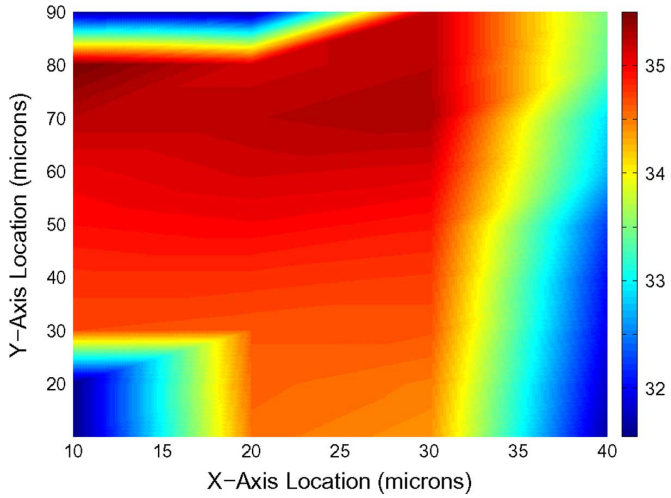

Fig. 14. PDMS well temperature for the front of the chip within 10 μm of the silicon dioxide surface.

temperature. These fluctuations had a larger effect on the temperature at the surface of the substrate than expected in the actual device due to coupling through the thermocouple. In addition, the size of the thermocouple was very large with respect to the scale of the measurements and had an additional affected the data. The data analyzed with a simple compensation for temperature. The temperature at the time of the measurement ($\mathrm{T_{amb}}$) was subtracted from the average temperature for all measurements, the average ambient temperature (T_{aa}). This value was subtracted from the temperature measured by the thermocouple (T_m) resulting in a compensated temperature equal to $T_m - (T_{aa} - T_{\mathrm{amb}})$. This is a simplified model for the effect of the fluctuations in ambient temperature on the measured temperature, but shows data more consistent with the simulations in Section V. In addition, the striations visible in the back side measurements are due to the manual scanning method employed to obtain data. Similar levels of striation were observed in plots for each of the planes parallel to the surface of the chip indicating that they were not generated by the chip itself, since the level of striation would decrease further from the chip if this were the case. The compensated temperature for the surface on the front side of the chip varies by 4 °C (Fig. 14) and the back side varies by 1.85 °C (Fig. 15). However, the compensation does not account for the presence of the thermocouple itself within the well. The measurements for the front side of the die clearly match the geometry of one corner of the heater. The measurements from the backside of the die are uniform except for the striations described. By comparing the results from both sides, it can be concluded that the silicon substrate's thickness and thermal conductivity are sufficient to evenly disperse the heat on the back surface.

VIII. Cell Culture

All work described in this section is done in a tissue engineering/cell-culture laboratory. This is available in all universities often as a shared research facility, and it includes basic analytical instrumentation, cold storage, centrifuge and laminar flow work areas. Standard procedures [1] were employed to sustain the cell line from which cells were harvested for the micro-incubator.

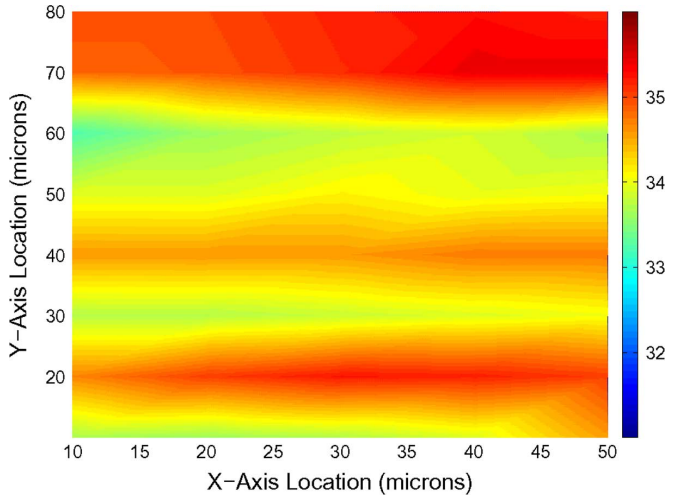

Fig. 15. Compensated PDMS well temperature for the back of the chip within 10 μm of the silicon surface.

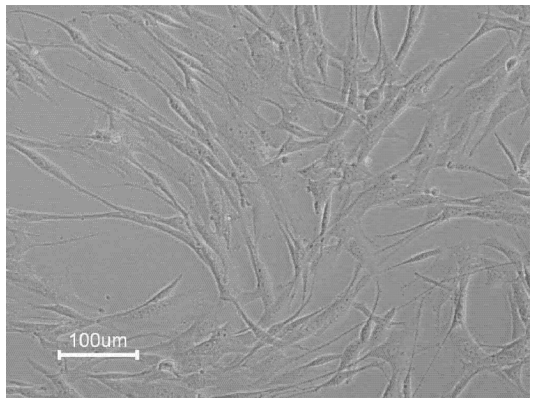

Fig. 16. Microphotograph of BHK-21 cells cultured using standard techniques and the protocol described in Section VIII. The morphology of the cells is used to comparatively assess the results of the described experimental cell work.

A. Materials and Methods

PBS 10x, pH 7.4 P313-000 was obtained from Biofluidics. Fibronectin, 0.1% solution, from bovine plasma (F1141), poly-D-lysine hydrobromide (P1024), collagen from rat tail powder, cell culture tested (C7661), and penicillin-streptomycin (P0781 100X, liquid, sterile-filtered, cell culture tested) were obtained from Sigma-Aldrich. Baby hamster kidney (BHK-21, CCL-10) cells were initially obtained from the American Type Culture Collection (Rockville, MD).

The cells were cultured in air-tight, sterilized tissue culture polystyrene flasks (Corning cell-culture flasks, 75 cm^2, angled neck, with phenolic cap, C7171) and maintained at 37 °C. Cells were subcultured at a density of 250 000–500 000 cells/mL using standard techniques with 0.05% trypsin in 0.53 mM EDTA. The culture media was composed of Minimum Essential Medium Eagle with Hank's Salts, 10% by volume FBS and 10-μL/mL penicillin–streptomycin.

The microphotograph in Fig. 16 shows healthy BHK-21 cells we successfully cultured as described. It is important to investigate the morphology since changes in the phenotype or poisoning, for instance, may not be detected as easily or early compared to assessment purely by proliferation rate. The morphology shown in the micrographs is typical of fibroblasts which are adherent (requiring an amenable surface over which they form a monolayer) and striated. Morphology, proliferation rate, and cell death were used as figures of merit for cell health and biocompatibility.

B. Biocompatibility and Adhesion Factor Testing

In designing a structure for cell culture, it is important to ensure that all the materials used are biocompatible and will not react with the media. The surface upon which the cells will grow is especially important since the cells must be able to attach to this surface. Adhesion factors are components of the extra cellular matrix (ECM) that act as ligands for some of the cell's surface receptors. Adhesion factors bind to most standard culture substrates. Glass is, of course, the most common substrate to which adhesion factors are applied. In fact, *in vitro* means literally "on glass." However, the glass used in traditional experiments has a slightly different composition than the passivation layer layer of a CMOS die (which varies from process to process), so it is prudent to ensure compatibility of the passivation layer. In addition, when performing fabrication steps that are not traditionally employed in cell culture such as those outlined in Section VI, it is important to ensure that the chemicals used in these processing steps do not leave behind residue that will affect the cells. Finally, the cleaning and sterilization processes for preparation of all the surfaces must be tested for compatibility to ensure they are sufficient.

In testing the materials for compatibility in cell culture, we tested for two different types of compatibility. The first was the ability for cells to successfully develop and divide in the presence of a material—general compatibility. The second, substrate compatibility, was the ability to use the material as a substrate for cell growth with or without the use of adhesion factors. Three common adhesion factors were tested: fibronectin, type I collagen and poly-D-lysine (PDL). Bio-compatibility tests were performed for each of the materials used in the micro-incubator, as well as, possible components for future generations of the system. Tests were performed on the following: a silicon wafer, silicon dioxide (an oxidized wafer), AMI die, MUMPS (MEMS) die, TSMC die, Peregrine SOS (silicon on sapphire) die, Dow Corning, Sylgard 184 (PDMS), General Electric RTV 615 (PDMS), and Kapton (polyimide) ribbon cable. The test results for both general and surface compatibility of the materials is shown in Table II. The results for materials coated with adhesion factors is shown in Table III.

C. Biocompatibility Test Protocol

All compatibility tests were performed in TPP 6-well tissue culture plates. General compatibility tests were performed by plating the cells on the bottom of the well in the tissue culture plate and adding a sample of the material to the well. Substrate compatibility tests were performed by placing the material in the well before plating then plating the cells directly onto the material. If adhesion factors were used, they were applied to the substrate as detailed below prior to introducing the substrate into the well. Each of the materials was washed with deionized (DI) water three times, ethanol, and phosphate buffered saline (PBS) twice, aspirating between, then dried in preparation for either the application of adhesion factors or if no adhesion factor was applied, introduction to the well. Each experiment was performed no less than three times in separate wells. Each plate

TABLE II
MATERIAL COMPATIBILITY TESTS—BIOCOMPATIBILTY TEST RESULTS

Material	General	Surface
silicon wafer	excellent	failed
oxidized wafer	excellent	good
glass coverslip	excellent	excellent
AMI die	excellent	failed
PDMS (Sylgard)	excellent	failed
PDMS (RTV615)	excellent	failed
polyimide ribbon cable	excellent	failed

TABLE III
ADHESION FACTOR SURFACE COMPATIBILITY TESTS—BIOCOMPATABILITY TEST RESULTS FOR ADHESION FACTOR COATED MATERIALS. WHILE MULTIPLE TESTS WERE PERFORMED FOR EACH CASE, THE RESULTS DID NOT DIFFER BETWEEN TESTS PER CASE. THE CONTROL FOR EACH TEST SHOWED NO SIGNIFICANT DIFFERENCE FROM CELLS CULTURED IN A STANDARD FLASK. N/A INDICATES THE COMBINATION WAS NOT TESTED

Material	Surface Comp. Fibronectin	Surface Comp. Type I Collagen	Surface Comp. Poly-D-lysine
silicon wafer	excellent	excellent	fair
oxidized wafer	excellent	excellent	fair
glass coverslip	excellent	excellent	excellent
AMI die	excellent	excellent	fair
MUMPS die	good	N/A	N/A
TSMC die	excellent	N/A	N/A
SOS die front	excellent	N/A	N/A
SOS die back	excellent	N/A	N/A
Sylgard	good	fair	failed
RTV615	good	fair	failed

used in the compatibility experiments had a well reserved for a control with no materials or adhesion factors added, the control for their respective experiment. The cells used for the control experiment were subcultured from the same vessel as the cells used in the experiment with the media and all other substances prepared in a single batch.

Assessment of the compatibility was performed by visual inspection and comparison of the cells to both cells cultured in standard tissue culture flasks and their control cells. Cell growth was assessed as excellent, good, poor, and failed. Results were obtain by observing cells after the time period for a normal growth cycle to reach the plateau phase. Excellent indicates confluent growth, good indicates high density, poor indicates low density, and failed indicates more than 50% cell death. All micrographs were taken after the cells were incubated for approximately 72 h.

Poly-D-lysine was prepared at a concentration of 0.1 mg/mL. The surface was flooded for 1h; excess was aspirated then rinsed with PBS, aspirated and allowed to dry. Fibronectin was prepared at 50 g/mL. The surface was flooded 1 h; tthe excess was aspirated, rinsed with minimum essential medium (MEM), aspirated, and allowed to dry. Collagen was diluted to 50 g/mL in 0.02 M Glacial Acetic Acid. The surface was flooded for 1 h; the excess was aspirated, rinsed twice with PBS, aspirated, and allowed to dry.

The silicon wafers were kept in the original shipping container, prior to biocompatibility experiments. The wafer used for the silicon dioxide coated wafer test was oxidized in the university's microfabrication facilities. A combination of wet and dry oxidation was used to create a silicon dioxide layer with a thickness of 1 μm with approximately 1 h of oxidation. The dies used

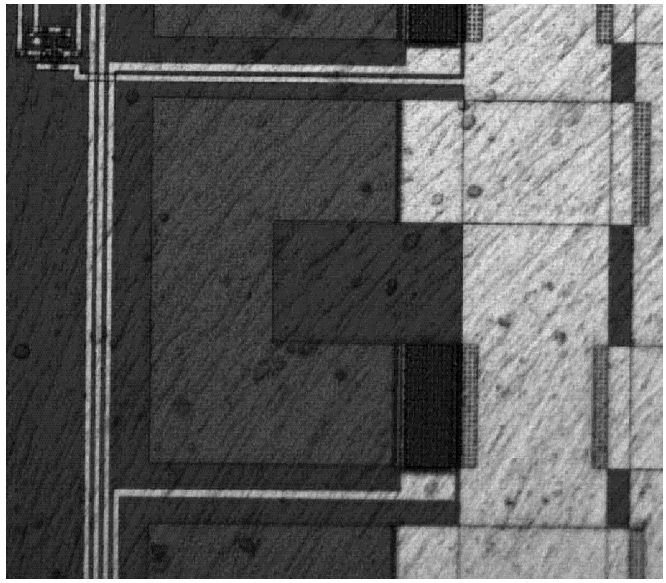

Fig. 17. Confluent cell growth on a CMOS die. The microphotograph is exemplary of the results from the surface compatibility tests. The result shown is from testing cell growth on an AMI die with fibronectin applied to the surface.

for testing were kept in the original shipping containers, but may have been removed for electrical testing using a probe station prior to testing. In several cases, this caused a small amount of damage to the surface of the die. The two brands of PDMS, Dow Corning Sylgard, and General Electric RTV615, were mixed at a 10:1 ratio as directed by the manufacturers and cured in a Blue-M oven at 100 °C overnight. Each of the materials was cleaned as described above.

D. Biocompatibility Test Results

The results of the compatibility tests [26] are summarized in Table II for general compatibility and Table III for surface compatibility. Successful cell culture on an AMI die is shown in Fig. 17. During testing of the PDMS well structure, we found that by applying the adhesion factor to either the entire well or limiting the adhesion factor to the substrate we could control the area of cell growth. We found that if the adhesion factor was applied to the entire well, the cells would spread over the sides of the well and grow onto the top surface of the PDMS well as shown in Fig. 18. This results was very important to the design of the micro-incubator. The area of cell growth is limited to the area to which the adhesion factor is applied.

E. Preparation of Cell Culture in the Microdevice

The microdevice was prepared for cell culture in a laminar flow hood dedicated to cell work. All surfaces and the interior of the micro-incubator were cleaned with either 70% ethanol or autoclaved before entering the hood. If ethanol is presented to the interior, it should be flushed twice with deionized water prior to preparation for culture. During any fluid transfer steps, if the positive and negative pressure applied to the PDMS network is not balanced, it can damage the device. The shape of the breathing layer indicates an imbalance in pressure by deforming into a convex or concave shape. If this imbalance is detected, the pressure can be easily corrected.

The adhesion factor, fibronectin, was applied to the cell-culture area by flowing only through the surface modification layer

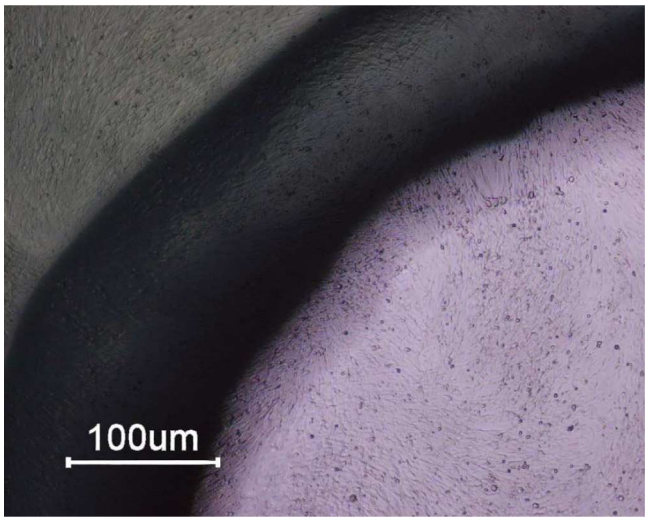

Fig. 18. Adhesion factor test for a PDMS well on glass substrate. The lightest area is the glass substrate, the black area is the sidewall of the PDMS well and the gray area is the top surface of the PDMS. Confluent cell growth is visible on each of the surfaces.

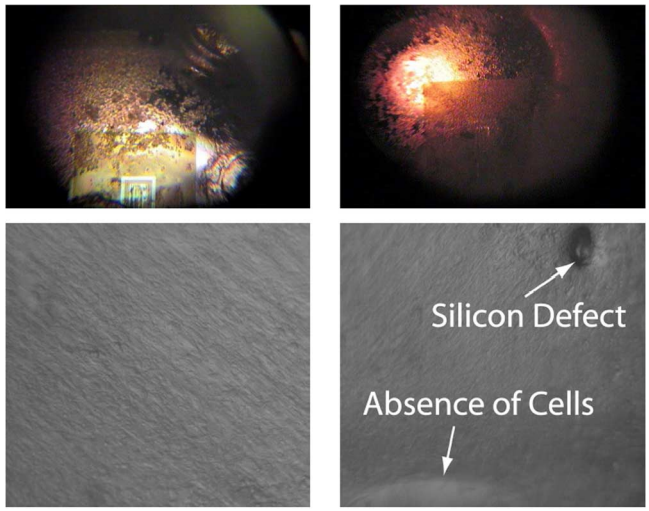

Fig. 19. Results for autonomous cell-culture and incubation using the fabricated microdevice. The first and second micrographs on top show results with the first generation chip that was used to culture cells on the front side of a die with temperature measured using a thermistor [21]. The first microphotograph (upper left) shows the micro-incubator after 42 h of incubation. The preferential cell growth away from the heater area is visible. The second microphotograph (upper right) shows the device at the conclusion of the experiment with 60 h of incubation. The third and fourth micrographs (bottom) show cell growth in the micro-incubator as described with cells cultured on the backside of the die. The temperature was measured with the PTAT circuit and heating was regulated by the PID control loop. The third and fourth microphotographs were taken after 72 h of incubation. While the majority of the substrate and area in the culture microvessel showed healthy cell growth (left), two areas with defects were detected and are shown (right).

channels. This step was important to ensure that cells did not adhere in the feeding layer when plated. Once the fibronectin was applied, the system was left to stand for 1 h. The system was then flushed with 1 mL of PBS. The system was then prepared for plating. At this point the cells can be introduced or the system can be stored at 4 °C for up to 3 days. Storage for periods longer than 3 days were not tested.

Prior to introduction into the micro-incubator, cells were resuspended in 1 mL of media and injected through the channels in the feeding layer. The syringes attached to the channels in the surface modification layer were kept attached during this process to maintain the pressure in these channels and prevent the media from entering these channels. After the cells were introduced, the system was allowed to rest for approximately 1 h to allow the cells to attach to the fibronectin coated glass at the bottom of the well. During this time the cells were present in the channels in the feeding layer, but did not attach due to the lack of the adhesion factor in this area. After the cells were attached to the bottom of the well, new syringes were attached to the feeding channels containing the appropriate media with FBS and antibiotics. The channels were flushed to remove any cells that were not attached, such as the cells that were present in the feeding channels. At this point the system was connected to the test setup for incubation. After 72 h of autonomous incubation, the cells were imaged as shown in Fig. 19; images from the first generation micro-incubator are shown for comparison.

IX. Discussion

A low-cost centimeter-scale disposable microdevice for cell-culture and incubation was demonstrated in this paper. In developing the microfluidic fabrication techniques, we have shown that fabrication of PDMS structures by replica molding is much more efficient than silicon electronics for several reasons. First, the master mold is reused throughout the process. The master mold is the only component that requires expertise, precision and expensive, complex equipment to fabricate. Since this master mold can be used almost indefinitely, it is practical to outsource the creation of the molds if the necessary facilities are not available. Once the master mold is completed numerous PDMS devices can be fabricated by simply pouring or spinning the PDMS onto the mold and curing. In silicon fabrication each layer requires expensive deposition techniques (oxidation, chemical vapor deposition, sputtering, etc.), photoresist deposition, lithography, photoresist development, etching, ashing, and several intermediate cleaning steps. Each of these steps must be repeated every time a new set of devices is created, making silicon devices not only more difficult and expensive to fabricated, but also consuming gallons of water and creating an enormous amount of chemical waste [27].

The risk of toxicity was decreased and fabrication efficiency increased by adding an extra processing step to the master mold fabrication. The photoresist-coated bases were used rather than plain silicon wafers, because this offers a simple technique to avoid adhesion of the PDMS to the surface of the mold without the use of any release agent. Several reasons motivated the use of this alternative approach. First, release agents can affect the surface of the PDMS making it more difficult for the molded PDMS to adhere to other surfaces. Second, release agents may be toxic to the cells or react with other chemicals used in experiments; decreasing the number of materials that will interact with biological materials simplifies biocompatibility testing. Finally, the use of release agents is a processing step that has to be repeated per layer, per device in the replica mold process while the blank base is a one-time per master mold fabrication step.

The use of multilevel PDMS in the design of the micro-incubator allowed for a more sophisticated design with elevated microfluidic channels for plating and feeding. This solves one

major problem in microfluidic cell-culture systems, sheer stress. Many of the passive PDMS cell-culture systems use complex feeding mechanisms [14] or structures [8] to decrease the flow rate and thus the sheer stress experienced by the cells. The system presented is designed so that the media is feed to the cells from an upper level so it enters the well from above rather than along the surface to which the cells attach, changing the direction of the stress. In addition to virtually eliminating sheer stress, this simple geometric modification results in a system that precludes the need for any automation in feeding the cells by mimicking the geometry of traditional cell-culture vessels. With the multilevel structure the media can be totally exchanged every few days in exactly the same manner as traditional cell culture using hand-operated syringes.

The architecture presented in this paper allows to use reflow in the channels with smaller cross-sectional area (the feeding layer microfluidic channels) to increase the device yield. It was empirically determined that reflowed positive masters provided viable devices more often than positive masters without reflow. Failure in PDMS layers created using positive masters occurred when the channels collapsed and sealed themselves shut during the assembly process.

The formation of air bubbles in the cell growth area was another problem that was solved through the use of a multilevel system. The presence of bubbles causes any cells in their interior to dry out and die. Bubbles also affect the flow of media through the channels and can increase the stress experienced by cells near the bubble by reducing the cross-sectional area of the flow path. In the multilevel system, the cells are not allowed to grow inside of the channel so if bubbles form in the channels they will have no effect on the cell growth. Since the well structure is not completely filled with media, but filled only to the height of the feeding channels, the bubbles that form in reservoir can be removed by gentle tapping that causes the bubble to rise to the surface of the media and dissipate. It was determined that bubbles were only formed in the well when the system was perturbed either by significant temperature changes or media exchange, as was the case in the channels. Thus, during steady state operation, there is no need to monitor the system for bubbles.

The use of a commercial CMOS process for fabricating the heater and the temperature sensor is a very important. Commercially available foundry processes are highly controlled and characterized. The necessary design tools such as model parameters, simulation kits and cell libraries are readily available for these processes. Integrated active electronic substrates with simple PDMS culture containers have been demonstrated in the past. The composite structures offering the greatest extent of capabilities is the use of a CMOS microchip [28], [29]. The microelectronic substrate opens up a wide variety of capabilities in stimulation, sensing and actuation, and the use of standard CMOS technology allows access to a vast wealth of cutting-edge electronic circuit designs. With the availability of small-volume and prototyping services [30], access to commercial fabrication facilities has become readily available eliminating the need for any in-house fabrication.

One of the most important advantages that miniaturization offers is portability. Innumerable biological assays would benefit from field or point-of-care analysis, e.g., biopsy tests. The elimination of expensive, bulky equipment also increases the accessibility of the technology to a wider population.

The use of active CMOS circuits for improved thermal sensing (PTAT circuit) and closed-loop control of the temperature was demonstrated via a software PID controller. Amplifiers and sensors to monitor electrical activity in the cell culture can also be included in the design [15], [29] in a more sophisticated data acquisition and monitoring system. Essentially, the fabrication of the silicon blocks for the micro-incubator or any other hybrid structure within the architecture presented does not require any in-house CMOS processing capabilities nor any custom circuit design capabilities.

Analysis and modeling of the structure is important to efficient design. In general multidomain modeling (fluidic, electrical, heat) is a challenging problem. Finite-element modeling is utilized here to perform complex 3-D analysis of the system. The simulations not only allow us to verify aspects of the system design that is very difficult to obtain through experimental means, but also allows us to vary system parameters without the need for custom fabrication that would be necessary for architecture exploration. Finally, by modeling not only the device, but also the packaging solutions the properties of the complete microsystem are studied as a whole. Through this modeling, it was demonstrated that polyimide ribbon cable packaging is preferable over a standard DIP (in addition to the biocompatibility and PDMS delamination concerns).

One of the most important aspects in the design of our system is that there is almost no deviation from the steps performs in traditional macroscale cell culture. The structure and use of the device is virtually the same as performing cell culture in a well-plate or flask and requires no more skill, difficulty or equipment than the basic cell-culture techniques. This is unique compared to previously published devices with complex heated perfusion systems. All of these elements combine to create a system that has unmatched ease of use and portability. The small device interfacing only a laptop computer with data acquisition board is not only ideal for field testing, but also gives a distinct advantage in a laboratory setting by allowing interface with equipment for constant electrical and optical observation, stimulation, and measurement while maintaining the incubation environment. This is an important aspect in that unheated systems and many perfusion systems either keep the cells constantly under stress or allow the cell to die during the testing phase which can significantly affect results. A testing environment much more representative of *in vivo* conditions combined with the simplicity of both the fabrication and use of the system and the virtually unlimited capabilities offered by the CMOS substrate result in a device with capabilities beyond any previously demonstrated.

Future designs, will explore the use of a transparent CMOS substrate. There are two methods that can be used to produce such a structure. The first is the use of the xenon difluoride etched chips [31], [32] on SOI-CMOS technologies. These structures are currently under investigation. The other method that involves silicon-on-sapphire CMOS (SOS-CMOS) process. A wireless heater and temperature sensor has been designed, fabricated and tested [33]. It will be tested in future design of the micro-incubator. The use of a transparent substrate will eliminate all of the imaging problems since the path from the cells to the microscope lens would be through the transparent substrate below the cells rather than the media and PDMS

TABLE IV
MATERIAL PROPERTIES: PART 1

	Young's Modulus(Pa)	Poisson's Ratio	Density(kg/m^3)
SiO_2	69×10^9[34]	0.17[34]	2200[35]
Silicon	190×10^9[36]	0.27[34]	2328[35]
Polysilicon	160×10^9[34]	0.2[34]	2331[34]
Aluminum	70×10^9[34]	0.3[34]	2697[34]
Gold	40×10^9[37]	0.44[37]	19300[38]
Copper	130×10^9[37]	0.34[37]	8890[38]
PDMS	500×10^9[37]	0.5[37]	0.97[37]
water	NA	NA	1000[39]
air	NA	NA	1.29[39]
Kapton	2.5×10^9[37]	0.32[40]	1420[37]

TABLE V
MATERIAL PROPERTIES: PART 2

	Thermal Expansion Coefficient $\left(\frac{1}{K}\right)$	Heat Capacity $\left(\frac{J}{kgK}\right)$	Thermal Conductivity $\left(\frac{W}{mK}\right)$
SiO_2	5×10^{-7}[35]	1000[38]	1.4[35]
Silicon	2.8×10^{-6}[34]	703[35]	148[34]
Polysilicon	2.8×10^{-6}[34]	703[35]	148[34]
Aluminum	23.1×10^{-6}[34]	900[38]	237[38]
Gold	14.2×10^{-6}[38]	130[38]	315[38]
Copper	16.6×10^{-6}[38]	390[38]	398[38]
PDMS	27×10^{-6}[41]	1460[37]	0.19[41]
water	NA	4184[39]	0.6[39]
air	NA	1000[39]	0.027[39]
Kapton	45×10^{-6}[42]	1090[37]	0.12[37]

above the cells. The micro-incubator thus could be readily used with standard inverted microscopes.

X. CONCLUSION

The combination of the techniques and methodologies presented in this paper allows for the development of scalable and cost effective methods of integrating basic CMOS integrated circuits with multilayer structures fabricated in soft silicone elastomer (PDMS) to control and manipulate liquids and gases. In the system design for an autonomous cell-culture and incubation microsystem, a commercially fabricated CMOS integrated circuit is employed for heating and sensing. The chip was integrated with multilevel PDMS microfluidic channels and reservoir to create the structures for culturing, testing and maintaining cells. Fabrication requires no special facilities or equipment (including plasma cleaning) other than a one time lithography step to create master replica molds for the PDMS channels. The steps involved in fabricating and assembling the structure employ simple "cookie-cutter" methods and "eyeball approximation." While a fair amount of manual work is involved in integrating the prototype system for research, **all processing and integration steps, are amenable to batch fabrication and integration**. Hence, the approach is viable for large scale industrial production and commercialization as a complete system or as component parts.

APPENDIX A

Tables IV–VI show material properties used in the finite element thermal analysis of Section V.

TABLE VI
MATERIAL PROPERTIES: PART 3

	Conductivity $\left(\frac{1}{\Omega m}\right)$	Refractive Index	Relative Permittivity
SiO_2	1.0×10^{-14}[22]	1.46[35]	3.9[35]
Silicon	1.0×10^{-12}[35]	3.42[38]	11.9[35]
Polysilicon	8.75×10^{-6}[35]	3.42[38]	11.9[35]
Aluminum	3.538×10^7[37]	1.44[37]	1.7[37]
Gold	0.410×10^8[38]	0.467[37]	6.9[37]
Copper	0.581×10^8[38]	0.25[37]	1[37]
PDMS	5.56×10^{-12}[41]	1.4[37]	2.7[37]
Kapton	0.666×10^{-15}[37]	1.7[37]	3.1[40]

ACKNOWLEDGMENT

The authors would like to thank F. Tejada for his assistance with wire bonding, P. Pouliquen and M. DiFredrico for their work on the data aquisition board, and J. Blain for her assistance with photography. They thank P. Jeff Wang for the use of his microscope and cell imaging system. CMOS chip fabrication was provided by MOSIS. The authors also thank Prof. M. Sachs, Director of the Whitaker Biomedical Engineering Institute and Prof. J. Elisseeff for graciously allowing the use of the shared tissue engineering laboratory in Clark Hall.

REFERENCES

[1] J. Davis, Ed., *Basic Cell Culture: A Practical Approach*, ser. A Practical Approach. New York: Oxford Univ. Press, 1994.
[2] Y. Xia and G. Whitesides, "Soft lithography," *Angewandte Chem. Inte. Ed.*, vol. 37, no. 5, pp. 550–575, Dec. 1998.
[3] S. Quake and A. Scherer, "From micro to nanofabrication with soft materials," *Science*, vol. 290, no. 5496, pp. 1536–1539, Nov. 2000.
[4] Fluidigm Corp. South San Francisco, CA, (2003) [Online]. Available: http://www.fluidigm.com/
[5] *Lab on a Chip*, Royal Society of Chemistry. Cambridge, U.K, 2001.
[6] A. Folch, B. Jo, O. Hurtado, D. Beebe, and M. Toner, "Microfabricated elastomeric stencils for micropatterning cell cultures," *J. Biomed. Mater. Res.*, vol. 52, no. 2, pp. 346–353, 2000.
[7] W. Gu, X. Zhu, N. Futai, B. Cho, and S. Takayama, "Computerized microfluidic cell culture using elastomeric channels and Braille displays," in *Proc. Nat. Acad. Sc.*, 2004, vol. 10, no. 45, pp. 15861–15866.
[8] E. Leclerc, Y. Sakai, and T. Fujii, "Cell culture in 3-dimensional microfluidic structures of PDMS (polydimethylsiloxane)," *Biomed. Microdev.*, vol. 5, no. 2, pp. 109–114, 2003.
[9] P. Hung, P. Lee, P. Sabounchi, N. Aghdam, R. Lin, and L. Lee, "A novel high aspect ratio microfluidic design to provide a stable and uniform microenvironment for cell growth in a high throughput mammalian cell culture array," *Lab on a Chip*, vol. 5, no. 44–48, pp. 44–48, 2005.
[10] N. Cohen, "The development of spontaneous beating activity in cultured heart cells: From cells to networks," Ph.D. dissertation, Israel Inst. Technol., Haifa, Israel, Dec. 2000.
[11] Applied Scientific Instrumentation. (2006) [Online]. Available: http://www.asiimaging.com.
[12] A. Tourovskaia, X. Figueroa-Masot, and A. Folch, "Differentiation-on-a-chip: A microfluidic platform for long-term culture studies," *Lab on a Chip*, vol. 5, pp. 14–19, 2005.
[13] A. Lambacher, M. Jenkner, M. Merz, B. Eversmann, R. Kaul, F. Hofmann, R. Thewes, and P. Fromherz, "Electrical imaging of neuronal activity by multitransistor-array (MTA) recording at 7.8 mm resolution," *Appl. Phys. A*, vol. 79, pp. 1607–1611, 2004.
[14] M. Shin, K. Matsuda, O. Ishii, H. Terai, M. Kaazemput-Mofrad, J. Borenstein, M. Detmar, and J. Vacanti, "Endothelialized networks with vascular geometry in microfabricated poly(dimethylsiloxane)," *Biomed. Microdev.*, vol. 6, no. 4, pp. 269–278, 2004.
[15] B. Debusschere and G. Kovacs, "Portable cell-based biosensor system using integrated CMOS cell-cartridges," *Biosens. Bioelectron.*, vol. 16, pp. 543–556, 2001.

[16] T. Wescott, "PID Without a Ph.D." (2000) [Online]. Available: http://www.embedded.com
[17] J. Charais, "Software PID control of an inverted pendulum using the PIC16F684," Microchip Technology Inc., Chandler, AZ, Appl. Notes 00964A, Oct. 2004.
[18] W. Zhou and W.-S. Hu, "On-line characterization of a hybridoma cell culture process," *Biotechnol. Bioeng.*, vol. 44, no. 2, pp. 170–177, Jun. 1994.
[19] S. Charati and S. Stern, "Difusion of gases in silicone polymers: Molecular dynamics simulations," *Macromolecules*, vol. 31, pp. 5529–5535, 1998.
[20] G. Walker, H. Zeringue, and D. Beebe, "Microenvironment design considerations for cellular scale studies," *Lab on a Chip*, vol. 4, pp. 91–97, 2004.
[21] J. B. Christen and A. Andreou, "Hybrid silicon/silicone (polydimethylsiloxane) microsystem for cell culture," in *Proc. IEEE Int. Symp. Circuits Syst.*, May 2006, pp. 2490–2493.
[22] COMSOL, Inc. Burlington, MA [Online]. Available: http://www.comsol.com/
[23] PageWorks, Cambridge, MA., (2001) [Online]. Available: http://www.pageworks.com
[24] Omega Engineering, Inc. Stamford, CT, 2006.
[25] Small Parts, Inc., Miami Lakes, FL, (2006) [Online]. Available: http://www.smallparts.com
[26] J. Blain Christen and A. Andreou, "CMOS heater array for incubation environment cellular study," in *Proc. 48th Midw. Symp. Circuits Syst.*, Aug. 2005, pp. 1786–1789.
[27] E. Williams, R. Ayres, and M. Heller, "The 1.7 kilogram microchip: Energy and material use in the production of semiconductor devices," *Environ. Sci. Technol.*, vol. 36, no. 24, pp. 5504–5510, Oct. 2002.
[28] M. Hutzler and P. Fromherz, "Silicon chip with capacitors and transistors for interfacing organotypic brain slice of rat hippocampus," *Eur. J. Neurosci.*, vol. 19, pp. 2231–2238, 2004.
[29] Y. Liu, E. Smela, N. Nelson, and P. Abshire, "Cell-lab on a chip: A CMOS-based microsystem for culturing and monitoring cells," in *Proc. 26th Annu. Int. Conf. Eng. Med. Biol. Soc. 2004,*, Sep. 2004, pp. 2534–2537.
[30] MOSIS, Marina Del Key, CA, (2006) [Online]. Available: http://www.mosis.org
[31] I. W. Chan, K. B. Brown, R. P. Lawson, A. M. Robinson, Y. Ma, and D. Strembicke, "Gas phase pulse etching of silicon for MEMS with xenon difluoride," in *Proc. 1999 IEEE Can. Conf. Elect. Comp. Eng.*, May 1999, pp. 1637–1642.
[32] J. B. Christen, C. Davis, M. Li, and A. Andreou, "Design, double sided post-processing, and packaging of CMOS compatible Bio-MEMS device arrays," in *Proc. IEEE Int. Symp. Circuits Syst.*, May 2002, vol. 1, pp. 665–668.
[33] E. Culurciello and A. Andreou, "3D integrated senseors in silicon-on-sapphire CMOS," in *Proc. 2006 IEEE Int. Symp. Circuits Syst.*, 2006, pp. 4959–4962.
[34] S. Senturia*, Microsystem Design*. Norwell, MA: Kluwer, 2001.
[35] S. Sze*, Physics of Semiconductor Devices*, 2nd ed. New York: Wiley, 1981.
[36] R. C. Jaeger*, Introduction to Microelectronic Fabrication*, ser. Modular Series on Solid State Devices, 2nd ed. Upper Saddle River, NJ: Prentice-Hall, 2002, vol. 5.
[37] C. Livermore and J. Voldman, "6.777J/2.751J Material Property Database," (2004) [Online]. Available: http://web.mit.edu
[38] S. A. Campbell, , A. S. Sedra, Ed.*, The Science and Engineering of Microelectronic Fabrication*, ser. The Oxford Series in Electrical and Computer Engineering, 2nd ed. New York: Oxford Univ. Press, 2001.
[39] H. T. Sensors, Thermal Conductivity Science (2006) [Online]. Available: http://www.hukseflux.com
[40] E. I. du Pont de Nemours and Company, DuPont Wilmington, DE, (2000) [Online]. Available: http://www2.dupont.com
[41] MG Chemicals, RTV Silicones by GE, Surrey, BC, Canada, (2006) [Online]. Available: http://www.mgchemicals.com
[42] G. Corp. Devon, PA [Online]. Available: http://www.goodfellow.com

Jennifer Blain Christen received the B.S., M.S., and Ph.D. degrees in electrical and computer engineering from The Johns Hopkins University, Baltimore, MD, in 1999, 2001, and 2006, respectively.

Her dissertation focused on a hybrid PDMS microfluidics/CMOS micro-incubator for autonomous cell culture. She held a graduate research fellowship from the National Science Foundation and a G K-12 fellowship also from the National Science Foundation. She is currently a Postdoctoral Fellow at the Johns Hopkins School of Medicine in the Immunogentics Department where she is working on a microfluidic platform for homogeneous (single strand) HLA (human leukocyte antigen) allele detection. Her broader research interests are in the design of analog and mixed-mode integrated circuits for direct interface to aqueous environments that incorporate biological materials and in bioelectronics.

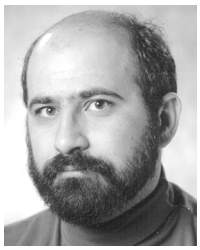

Andreas G. Andreou received the Ph.D. degree in electrical engineering and computer science in 1986 from The Johns Hopkins University, Baltimore, MD.

Between 1986 and 1989, he held Postdoctoral Fellow and Associate Research Scientist positions in the Electrical and Computer Engineering Department while also a member of the professional staff at the Johns Hopkins Applied Physics Laboratory, Johns Hopkins University, Baltimore, MD. He became an Assistant Professor of Electrical and Computer engineering in 1989, Associate Professor in 1993, and Professor in 1996. He is also a Professor of Computer Science and of the Whitaker Biomedical Engineering Institute and director of the Institute's Fabrication and Lithography Facility in Clark Hall. He is the Co-Founder of the Johns Hopkins University Center for Language and Speech Processing. Between 2001 and 2003, he was the Founding Director of the ABET accredited undergraduate Computer Engineering program. In 1996 and 1997, he was a Visiting Professor of the computation and neural systems program at the California Institute of Technology, Pasadena. During the summer of 2001 he was a Visiting Professor in the Department of Systems Engineering and Machine Intelligence at Tohoku University, Japan. His research interests include sensors, micropower electronics, heterogeneous microsystems, and information processing in biological systems. He is a Co-Editor of the *Low-Voltage/Low-Power Integrated Circuits and Systems* (translated in Japanese) (IEEE Press, 1998) and *Adaptive Resonance Theory Microchips* (Kluwer, 1998).

In 1989 and 1991, Dr. Andreou was awarded the R.W. Hart Prize for his work on mixed analog/digital integrated circuits for space applications. He is the recipient of the 1995 and 1997 Myril B. Reed Best Paper Award and the 2000 IEEE Circuits and Systems Society, Darlington Best Paper Award. In 2006, he was elected as an IEEE Fellow and a Distinguished Lecturer of the IEEE Electron Devces Society (EDS). He is currently an Associate Editor of IEEE TRANSACTIONS ON CIRCUITS AND SYSTEMS—I: REGULAR PAPERS.